Wintertime storage of water in buried supraglacial lakes across the Greenland Ice Sheet

L.S. Koenig[1,2*], D.J. Lampkin[3], L.N. Montgomery[3], S.L. Hamilton[4], C.A. Joseph[3], S.E. Moutsafa[5], B. Panzer[6], K.A. Casey[7,1], J.D. Paden[6], C. Leuschen[6] and P. Gogineni[6]

[1]{Cryospheric Sciences Laboratory, NASA Goddard Space Flight Center, Greenbelt, MD}

[2]{now at National Snow and Ice Data Center, University of Colorado, Boulder, CO}

[3]{Department of Atmospheric and Oceanic Sciences, University of Maryland, College Park, MD}

[4]{Bowdin College, Brunswick, ME}

[5]{Department of Geography, Rutgers, The State University of New Jersey, Piscataway, NJ}

[6]{Center for Remote Sensing of Ice Sheets, University of Kansas, Lawrence, KS}

[7]{Earth System Science Interdisciplinary Center, University of Maryland, College Park, MD}

Correspondence to: L.S. Koenig (lora.koenig@colorado.edu)

Abstract

Increased surface melt over the Greenland Ice Sheet (GrIS) is now estimated to account for half or more of the ice sheets total mass loss. Little, however, is known about the complex supra-, en- and subglacial hydrologic systems that transport the melt across and through the ice sheet to the ocean. Here, we show that some melt water is stored, over-winter in buried supraglacial lakes. Airborne radar is used to detect these buried lakes distributed extensively around the margin of the GrIS from 2009 to 2012. The subsurface water can persist through multiple winters and is, on average, ~1.9 + 0.2 m below the surface. The few buried lakes that are visible on the surface of the GrIS have a unique visible signature associated with a darker blue color where subsurface water is located. The volume of retained water in the buried lakes is likely insignificant compared to the total mass loss from the GrIS but the water

will have important implications locally for the development of the englacial hydrologic system and ice temperatures. The buried lakes represent a small but year-round source of meltwater in the GrIS hydrologic system.

1 Introduction

Annual mass loss from the Greenland Ice Sheet (GrIS) has substantially increased, quadrupling, in the last two decades (Shepherd et al., 2012). Warming Arctic temperatures (e.g. Comiso, 2003; Hall et al., 2013) and a decrease in ice sheet albedo (e.g. Angelen et al., 2014; Box et al., 2012; Tedesco et al., 2011) have increased surface melt which now accounts for half or more of the total mass loss, outpacing ice dynamics in recent years (van den Broeke et al., 2009; Enderlin et al., 2014; Khan et al., 2014). Even with the increasing GrIS surface melt, highlighted by a record melt and runoff event in 2012 (Nghiem et al., 2012; Hall et al., 2013; Hanna et al., 2012), the supra-, en- and subglacial transport of the melt water is still relatively unknown, unquantified and not simulated in surface mass balance models (Rennermalm et al., 2013).

Quantifying supra-, en- and subglacial transport and routing of melt water is of particular importance to better understand and constrain modeled estimates of runoff volume and timing and to improve projections of future sea level rise (SLR) (Rennermalm et al., 2013). While regional climate models agree relatively well (~20% variation) on precipitation amounts across the GrIS, they still have large discrepancy (from 38-83% variance) in melt production, refreeze, and runoff (Vernon et al., 2013) due, not only to differences in the models, but also due to a general lack of field observations quantifying melt water retention, transport and runoff (Rennermalm et al., 2013). Field observations have only recently discovered large amounts of water retention (Forster et al., 2013; Koenig et al., 2014) and latent heating from refreeze (Harper et al., 2012; Humpherys et al., 2012) on the perimeter of the GrIS and model improvements to account for the water retention are still in their initial stages (Kuipers Munneke et al., 2014). These recent discoveries punctuate that more observations are needed of the GrIS hydrologic system to fully understand melt water transport and eventual runoff.

This paper presents an initial study and mapping of over-winter surface melt retention in buried supraglacial lakes (Figure 1) within the GrIS. Referred to here simply as buried lakes and defined as water retained through a winter season at shallow depths within the ice sheet that originally formed, during a previous melt season, as a supraglacial lake. Thus, a buried lake is a specific type of supraglacial lake that spans the boundary between the supra- and englacial hydrologic system; existing under lake ice and snow/firn layers in some seasons and reemerging as a supraglacial lake in others. Near-surface, high resolution radar data, collected during the Arctic Spring Campaigns of Operation IceBridge (OIB), clearly show water retention in buried lakes through the winter season and are used to map their extent and depth. Buried lakes provide an example of a year round latent heat source (Humphreys et al., 2012; Kuiper Munneke et al., 2014) currently unaccounted for as well as a year round source of melt water, substantiating hydrologic discharge measurements showing that the GrIS hydrologic system remains active even during the cold winter months (Rennermalm et al., 2013).

2 Background

Several have studied supraglacial lakes, which are easily distinguishable by visible and radar satellites, when they form seasonally in the ablation and percolation zones across the GrIS (Echelmeyer et. al., 1991; Box and Ski, 2007; McMillan et al., 2007; Sneed and Hamilton, 2007; Sundal et al, 2009; Lampkin, 2011; Selmes et al., 2011; Tedesco and Steiner, 2011; Howat et al., 2013). Supraglacial lakes form in local topographic lows formed by bedrock depressions, which are not advected by the ice, and often reform in the same locations (Echelmeyer et al., 1991; Box and Ski, 2007; Selmes et al, 2011). Das et al., (2008) observed the rapid (< 2 hours) drainage of a supraglacial lake through fractures, delivering surface meltwater to the bedrock-ice interface causing local uplift and glacier acceleration. (van der Veen, 1998; Alley et al., 2005; van der Veen, 2007; Krawczynski et al., 2009). Further studies expanded the links between supraglacial lakes, and water filled crevasses, to the en- and subglacial hydrologic system, clearly showing that surface meltwater routes to the bed of the GrIS causing a dynamical increase in ice velocity to some threshold value. (Zwally et al., 2002; Joughin et al., 2008; Catania et al., 2008; Bartholomew et al., 2011; Palmer et al., 2011; Sundal et al., 2011; Hoffman et al., 2011; Tedstone et al., 2013).

Most studies assume that supraglacial lakes either drain during the summer, through the supraglacial or englacial hydrologic system, or refreeze during the winter. Few studies have investigated the behavior of supraglacial lakes during the winter season. Ohmura et al. (1991), however, observed and reported the presence of ice plates on the snow surface at West Lake near Swiss Camp in Western Greenland. They attributed the ice plates to the persistent of water late into winter which formed a frozen ice layer and then drained. Additionally, they detected a deep lake (~10 m) to the east of Swiss Camp that likely remained water filled through the winter developing lake ice up to 1.5 m thick before draining in spring or early summer. Rennermalm et al. (2013) also showed evidence of water retention, somewhere within the GrIS hydrologic system, from peaks in stream discharge occurring in the fall and spring, up to 6 month after surface melt.

There has not been a systematic assessment of the extensive high-resolution radar data (first provided by OIB in 2009) to confirm wintertime storage of water in supraglacial lakes or to map the spatial and temporal distribution. This effort is the first to characterize wintertime meltwater storage in buried lakes over the GrIS and provide an assessment of its impact on the hydrologic system.

3 Data

3.1 Radar data

Radar data acquired from the CReSIS ultra-wideband Snow Radar (Leuschen, 2014) during OIB Arctic Campaigns from 2009 through 2012 are used to identify subsurface water. The radar operates over the frequency range from ~2 to 6.5 GHz where water has a high absorption coefficient resulting in the attenuation of radar waves and a strong reflection of the wave at the ice-water interface due to the large difference between the dielectric constant of ice and water (Figure 2) (Ulaby et al., 1981). The Snow Radar uses a Frequency Modulated Continuous Wave (FMCW) design which provides a vertical resolution of ~ 4 cm in snow/firn to a depth of tens of meters. Radar backscatter along a transect is often displayed as an echogram (Figure 2) which provides a visual image of the subsurface returns. For additional details on the Snow Radar performance see Panzer et al. (2013) and Rodriguez-Morales et al. (2014).

3.2 Visible and thermal imagery

Visible imagery is used from several imaging platforms to support the analysis of buried lakes. OIB Digital Mapping System (DMS) imagery, acquired coincident with Snow Radar data, is used to examine surface features indicative of the presence of subsurface water. Cloud-free Moderate Resolution Imaging Spectroradiometer (MODIS) Rapid Response Arctic Subset true color imagery (250 m resolution) are used to determine if supraglacial lakes formed previously at the location of the buried lakes. Additionally, at a sample lake site, MODIS Land Surface Temperature (LST) data are used to corroborate melt onset and surface thermal conditions along with Landsat, Enhanced Thematic Mapper (ETM+) panchromatic imagery, with a resolution of ~15 m, to evaluate the summertime evolution of the lake.

DMS acquires imagery in the visible part of the electromagnetic spectrum at a nominal resolution of 10 cm (at 1500 feet AGL, the nominal OIB flight altitude). DMS collects data over three multispectral and panchromatic bands using a 21 megapixel Canon EOS 5D Mark II digital camera. Data are orthorectified and corrected for camera orientation using the Applanix POS/AV navigation system. For additional details see Dominguez (2014).

MODIS LST (MOD11A1, version 5.1) swath data at 1 km resolution are accurate to within ± 1°C (Wan et al., 2002; Hall et al., 2008) for snow and ice surface temperatures between -15 to 0°C (Hall et al., 2008). MODIS LSTs acquired over the GrIS, however, can be ~1 to 3 degrees colder than the actual surface temperatures (Hall et al. 2013; Koenig and Hall, 2010).

4 Methods

4.1 Detection of buried lakes from airborne radar

All Snow Radar echograms over the GrIS from 2009-2012 were manually inspected for subsurface attenuations of the radar backscatter, possibly attributed to a buried lake (Figure 2B). To ensure the radar response was associated with englacial water, and not some other density or dielectric change, all 2011 detections from Snow Radar data were compared to either the Accumulation Radar (~600-900 MHz) or MCoRDS Radar (~140-260 MHz), flown simultaneously with the Snow Radar onboard the OIB aircraft (Figure 2). Water attenuates across radar frequencies. If at least one additional radar showed attenuated backscatter the detection remained in the dataset. Additionally, all detections were compared to summertime cloud-free MODIS imagery to confirm that a supraglacial lake formed at the buried lakes location during a melt season (Figure 3). The 2011 Snow Radar data were chosen for this initial analysis because it was the first year in which the OIB radar operators discovered the unique return over supraglacial lake regions.

The analysis of the 2011 Snow Radar data led to two characteristic echogram patterns for englacial water retention: buried supraglacial lakes (Figure 2B) and water-filled crevasse fields. The water-filled crevasse fields were not included in the analysis presented here because, though it is likely they contain englacial water, it is also possible that the crevasses, or hoar crystals formed within them, are scattering the radar signal causing a similar backscatter signature to subsurface water. Additional field verification is needed to confidently interpret radar backscatter over crevassed regions.

The buried lake detections from 2011 were mapped using approximately the center point of the feature and were compared to high resolution (cm-scale) DMS imagery of the GrIS surface coincident with the radar collection (Figure 4) (Dominguez, 2014). DMS imagery is used to visually characterize the surface roughness, detect crevasses and to look for any distinct surface expression of the buried lakes.

Finally, to construct a time series of buried lakes, the characteristic buried-lake radar return (Figure 2B), determined from the 2011 data, were used to map buried lakes from the 2009, 2010 and 2012 Snow Radar data. Buried lakes that formed within 1 km of each other from year-to-year are considered the same feature. Selmes et al. (2011) reported a median area of 0.56 km^2 and a mean area of 0.80 km^2 for lakes across the GrIS. Because the buried lakes are mapped using an approximate center point, a 1 km radius is a reasonable distance to be considered the same feature along the changing OIB flight lines.

4.2 Depth retrieval of the water surface

The 2009-2012 Snow Radar echograms of the buried lakes were manually digitized to determine the depth from the snow surface to the water surface. If distinguishable in the echogram, as shown in Figure 2B, both the snow-lake ice interface and the lake ice-water interface were digitized. When a snow layer is digitized, a constant density of 320 kg/m^3, a reasonable density estimate for the top meters of snow across the GrIS (Benson, 1962), is used to convert radar travel time to depth using equations developed by Wiesmann and Matzler (1999). When a lake ice layer is digitized or if only the snow surface and the water layer are digitized, the dielectric properties of ice are assumed to convert radar travel time to depth (Dowdeswell and Evan, 2004). In the absence of field data providing a stratigraphic density profile, the ice assumption is made which biases the depth measurements to shallower depths. The uncertainties in the depth are estimated by taking the subset of radar echograms where a snow layer was detected and calculating the depth with both the snow layer and ice assumptions. The average percent difference defines the uncertainty at 10% (range of 2% to 26%) shallow because radar waves travel slower in solid ice than snow/firn which contains more air.

5 Results

5.1 Spatial and temporal distribution of buried lakes

The wintertime storage of meltwater in buried lakes is extensive around the margin of the GrIS (Figure 5). All buried lakes identified from 2009-2012 were below the 2000 m contour of the GrIS with the majority falling between 1000 m and 2000 m on the west coast of the ice sheet (Figure 5). Table 1 provides the number of buried lakes detected each year, the mean and standard deviation of buried lake elevation, the number of buried lakes below 1000 m and the number of lakes detected per 1000 km of OIB flight lines flown below 2000 m. Because OIB is an airborne mission with a changing set of flight lines leading to an inconsistent spatial sampling, and thus regionally biased sampling, results must be analyzed with caution. In Table 1 it appears that more lakes were detected in 2011 but there were also more flightlines in 2011 below 2000 m many along the west coast.

Clusters of buried lakes are concentrated along the west coast of Greenland and near 79 N and Zachariæ Isstrøm where OIB gridded flight lines are flown repeatedly in multiple years (Figure 5). It is also in these regions where we detect buried lakes that persist for multiple years (Figure 5). Again, these multi-year detections must be taken in context, they occur in areas with high concentrations of supraglacial lakes where OIB flightlines are repeated in multiple years. It is very likely that other buried lakes are present through multiple winters that are not being detected due to the limited OIB spatial and repeat sampling. In total 53 lakes were detected in 2 of the 4 years and 7 lakes were detected in 3 of the 4 years (Figure 5). All lakes detected over three seasons are located on the OIB grid near Jakobshavn Isbræ that is repeated annually.

5.2 Surface expression of buried lakes and lake evolution

DMS imagery rarely shows any surface expression of the buried lake (Figure 4). At five locations, however, a unique surface expression was found when the buried lake’s ice covered surface was exposed (examples from two of the buried lakes shown in Figures 4 and 6). These figures show relatively darker blue ice adjacent to a region of lighter colored ice that corresponds with the transitional zone from water detection (attenuation) to no water detection (penetration) in the radar echograms (Figures 4 and 6). While scattering and absorption of visible light over buried lakes is indeed complex with snow, water, lake ice and glacial ice (Grenfell and Perovich, 1981; Warren, 1984), the darker blue color associated with retained water can be explained by the vibrational transitions as well as the higher density and temperature of water molecules in the buried lake liquid water resulting in stronger hydrogen-oxygen bond absorption feature near 600 nm. Simply, the hydrogen bonds in liquid water cause a shift to lower energy over ice which would produce the darker blue color (Luck, 1980; Langford et al., 2001). Unfortunately the DMS data used here cannot directly quantify the spectral signature of the lighter and darker blue colors associated with no retained water and retained water, respectively, and is left for future work with high resolution satellite imagery.

Figure 6 shows a radar echogram and DMS image of a lake detected on May 2, 2011, approximately 100 km inland from the terminus of 79 N Glacier in Northern Greenland. Radar backscatter clearly shows melt on the surface (Figure 6 between locations 3 and 4) likely driven by radiative heating. The rest of the frozen lake (Figure 6 between locations 1 and 2) and buried lake (Figure 6 between locations 2 and 3) has persistent accumulated snow insulating the ice underneath preventing the onset of melt. Landsat ETM+ images during the peak of the 2011 melt season (Figure 7) demonstrate that lake extent corresponds to regions in the radar echogram where melt was initiated (Figure 7 between locations 3 to 4) and that the region of the buried lake (Figure 7 between locations 2 and 3) maintained a floating ice cap into the melt season. MODIS LST data, the only temperature data available for this site and date, show a peak temperature of -10.7 C during the 1640 GMT overpass. The Snow Radar and DMS data were acquired at 1609 GMT when OIB overflew the site very close to the peak temperature and solar input. The MODIS LST, however, is rather low for the production of water observed in the echogram over this site which is probably the result of the relatively coarse spatial resolution (1 km) of MODIS such that the very small patch of surface melt, or melt from a few cm below the surface, at the edge of the lake was not resolved. The evolution of this particular buried lake into the melt season is concentrated melting around the perimeter of the lake while the deeper center of the lake remains insulated with a floating cap, likely increasing the probability it will persist throughout the next winter season barring some supra- or englacial drainage event. This data also indicates that the early onset of melt is spatially heterogeneous primarily occurring at locations where darker ice is exposed and that some of the first melt of the season is associated with exposed buried lakes.

5.3 Depth distribution of buried lakes

Figure 8 shows a histogram of the digitized water layer depths from every radar return over a buried lake. The average depth to the retained water during the April and May OIB flights from 2009 to 2012 is 1.88 +0.16 m with a total range of 0.05 +0.01 m to 9.43 +0.85 m and a standard deviation of 1.30 m. There is not a distinctive pattern in buried lake depths along the margins of the GrIS. 38% of radar returns delineated a snow layer above the lake ice with an average snow layer thickness over the buried lakes of 0.65 m (range of 0.15 m to 2.93 m) and an average ice layer thickness below the snow of 1.40 m (range of 0.4 m to 4.58 m). Uncertainties associated with estimates of density stratigraphy across the GrIS, which is used to convert radar travel time to depth, likely cause a shallow bias in these depth measurements of on average 9% and up to 24%. Nonetheless, our estimates provide the first initial determination of the depth of stored water in buried lakes below the surface of the GrIS as well as constrain the thickness of lake ice that forms over the buried lakes.

6 Discussion

6.1 Buried lakes and surface mass budget

Though the water stored in buried lakes is spatially extensive it is a very small amount of mass that likely has little influence on mass loss projections for Greenland. Assuming all the buried lakes detected in 2011, the year with the maximum number of lakes, were the size of the mean supraglacial lake detected by Selmes et al. (2011) with a large water depth of 10 m, the volume of water retained in the lakes would amount to ~1.5 Gt of water over an area of ~ 140 km^2. For comparison the englacial storage of water in the firn aquifer, recently discovered in Southeast, Greenland is estimated to cover an area of ~70,000 km^2 with ~140 Gt of water (Forster et al., 2013; Koenig et al., 2014). Models, which have large inter-annual and inter-model variance, estimate total GrIS runoff between 100 to 300 Gt annually (Vernon et al., 2013). Though the amount of water stored is likely insignificant, the spatial distribution of the retained water is locally important for the development of the hydrologic system and ice temperatures.

6.1 Lake evolution and implications for the hydrologic cycle

A buried lake represents a newly documented and mapped feature in the evolution of a supraglacial lake. Once formed a supraglacial lakes can 1) drain through the englacial or supraglacial hydrologic system sometime throughout the year, 2) refreeze completely during the winter season or 3) partially freeze during the winter season, form lake ice and retain water at depth becoming a buried lake. Buried lakes can resurface in the following melt season or remain buried for multiple seasons before remerging at the surface. As shown in Figure 7, many of the reemerging lakes have a characteristic crescent or toroid shape and maintain a floating ice cap into the melt season. The formation of buried lakes on the GrIS follows the natural wintertime evolution of lake ice formation over Arctic lakes on land, with similar ice thicknesses ranging between 1 and 2 m, (e.g. Surdu et al., 2014) as well as the same pattern of meltpond refreezing on sea ice, creating trapped ponds until complete refreeze is accomplished (Flocco et al., 2015). Satellite images of the summertime extent of the supraglacial lakes paired with the subsurface radar data shown here suggest that at elevations above 1000 m all three types of supraglacial lakes coexist in the same region, all experiencing the same meteorological forcings. How and which supraglacial lakes become buried lakes, is still unanswered but a discussion of possible formation mechanisms and evolution is warranted.

The initial formation of a buried lake is likely dependent on two factors 1) the degree of connectivity of the lake to the supra- and englacial hydrologic system responsible for the transport of water out of the lake and 2) the water volume stored in the lake at the end of the melt season, particularly the depth, which determines the energy balance required to freeze. Without further research and modeling it is unclear if either connectivity or depth is a more dominate factor in predicting buried lakes formation but with increasing melt extent across the GrIS (Mote et al, 2007; Nghiem et al., 2012; Hall et al., 2013) both may increase over time.

When a buried lake reaches the surface, and thaws, it will initially contain a larger amount of water in the lake basin than a neighboring drained basin at the start of the melt season. As the season progresses less melt water will be needed to fill the already partially filled basin. A more efficient filling of the lake basin would lead to more efficient overtopping and surface overflow, eventually leading to the development of supraglacial channels. Buried lakes tend to be prevalent at elevations coincident with the occuence of lake associated with more than one outflow channel (Lampkin et al., 2013). It is, therefore, possible buried lakes, overtime, promote supraglacial channel development leading to a more connected lake basin, diminishing the chances of a buried lake forming in subsequent seasons. More research is needed but if this scenario is true, a buried lake may be a transient process in the development of a more efficient hydrologic system.

The retained water in buried lakes will also warm ice locally at the surface of the ice sheet as measured and modeled by Humphreys et al. (2012) and Kuiper Munneke et al. (2014). If the buried lake water infiltrates cracks at the base of the lake it is capable of delivering meltwater, and its associated latent heating, deeper into the ice sheet. The resultant heating and softening of the ice could affect ice flow dynamics, especially if concentrations of buried lakes are located at lateral margins of outlet glaciers. The rise in ice temperatures around conduits would also make it easier to activate the conduit in the spring/summer which supports the hypothesis the buried lake are part of the evolutionary cycle towards a more efficient drainage system. Considering this mechanism buried lakes provide a possible water source for the peaks in stream discharge observed by Rennermalm et al. (2013) when no surface melt was present. Buried lakes represent a mechanism to extend surface melt water infiltration deeper into the GrIS at anytime during the year.

7 Conclusions

Buried lakes are extensively distributed around the margins of the GrIS. A few previous studies suggested that water remained in the supraglacial lakes late into the winter season; however, these data are the first to confirm and extensively map the distribution of the retained water. Though the water retained in buried lakes is insignificant compared to total mass loss, it has important implications for the local temperature profile, development of the englacial hydrologic network and ice dynamics. This research presents a new understanding of meltwater routing through and within the GrIS and emphasizes the need to better understand the hydrologic pathways through which meltwater drains toward the ocean. Ultimately, understanding surface melt and supraglacial lake water storage and drainage will lead to a better understanding of how the increases in the GrIS mass loss from surface melt contribute to SLR over time.

Acknowledgements

The authors thank L. Brucker and T. Neumann for their insightful discussions. This work was supported by the NASA’s New Investigator and Cryospheric Sciences Programs. Data collection and instrument development were made possible by The University of Kansas’ Center for Remote Sensing of Ice Sheets (CReSIS) supported by the National Science Foundation and Operation IceBridge. S.E.M supported by NASA’s Earth and Space Science Fellowship Program grant NNX12AN98H.

References

Alley, R. B., Dupont, T. K., Parizek, B. R. and Anandakrishnan, S.: Access of surface meltwater to beds of sub-freezing glaciers: preliminary insights, Ann. of Glac., 40, 8–14, 2005.

Angelen, J. H., Broeke, M. R., Wouters, B., & Lenaerts, J.: Contemporary (1960-2012) evolution of the climate and surface mass balance of the greenland ice sheet. Surveys in Geophysics, 35(5), 1155-1174. doi:http://0-dx.doi.org.libraries.colorado.edu/10.1007/s10712-013-9261-z, 2014.

Bartholomew, I., Nienow, P., Sole, A., Mair, D., Cowton, T., Palmer, S. and Wadham, J.: Supraglacial forcing of subglacial drainage in the ablation zone of the Greenland ice sheet, Geophys. Res. Lett., 38, doi:10.1029/2011GL047063, 2011.

Benson, C. S.: Stratiraphic studies in the snow and firn of the Greenland Ice sheet. SIPRE Res. Rep. 70, 1962.

Box, J. E. and Ski, K.: Remote sounding of Greenland supraglacial melt lakes: implications for subglacial hydraulics, J. Glaciol., 53(181), 257–265, doi:10.3189/172756507782202883, 2007.

Box, J. E., Fettweis, X., Stroeve, J. C., Tedesco, M., Hall, D. K., & Steffen, K.: Greenland ice sheet albedo feedback: Thermodynamics and atmospheric drivers. The Cryosphere, 6(4), 821, 2012.

Van den Broeke, M., Bamber, J., Ettema, J., Rignot, E., Schrama, E., van de Berg, W. J., van Meijgaard, E., Velicogna, I. and Wouters, B.: Partitioning Recent Greenland Mass Loss, Science, 326, 984–986, doi:10.1126/science.1178176, 2009.

Catania, G. A., Neumann, T. A. and Price, S. F.: Characterizing englacial drainage in the ablation zone of the Greenland ice sheet, J. Glaciol., 54(187), 567–578, doi:10.3189/002214308786570854, 2008.

Comiso, J. C.: Warming Trends in the Arctic from Clear Sky Satellite Observations, J. Clim., 16(21), 3498–3510, doi:10.1175/1520-0442, 2003.

Das, S. B., Joughin, I., Behn, M. D., Howat, I. M., King, M. A., Lizarralde, D. and Bhatia, M. P.: Fracture propagation to the base of the Greenland Ice Sheet during supraglacial lake drainage., Science, 320(5877), 778–81, doi:10.1126/science.1153360, 2008.

Dominguez, R.: IceBridge DMS L1B Geolocated and Orthorectified Images, Boulder, Colorado, NASA DAAC at the National Snow and Ice Data Center, accessed 2014.

Dowdeswell, J. A. and Evans, S.: Investigations of the form and flow of ice sheets and glaciers using radio-echo sounding, Rep. Prog. Phys., 67(10), 1821–1861, doi:10.1088/0034-4885/67/10/R03, 2004.

Echelmeyer, K., Clarke, T. S. and Harrison, W. D.: Surficial glaciology of Jakobshavn Isbræ, West Greenland 1. Surface-morphology, J. Glaciol., 37, 368–382, 1991.

Flocco, D., Feltham D. L., Bailey, E. and Schroeder, D.: The refreezing of melt ponds on Arctic sea ice, J. Geophys. Res. Oceans, 120, doi:10.1002/2014JC010140, 2015.

Forster, R. R., Box, J. E., van den Broeke, M. R., Miège, C., Burgess, E. W., van Angelen, J. H., Lenaerts, J. T. M., Koenig, L. S., Paden, J., Lewis, C., Gogineni, S. P., Leuschen, C. and McConnell, J. R.: Extensive liquid meltwater storage in firn within the Greenland ice sheet, Nat. Geosci., 7(2), 95–98, doi:10.1038/ngeo2043, 2013.

Grenfell, T. C. and Perovich, D. K.: Radiation absorption-coefficients of polycrystalline ice from 400-1400 nm, J. Geophys. Res. Atmos., 86(NC8), 7447–7450, doi:10.1029/JC086iC08p07447, 1981.

Hall, D. K., Box, J. E., Casey, K. A., Hook, S. J., Shuman, C. A. and Steffen, K.: Comparison of satellite-derived and in-situ observations of ice and snow surface temperatures over Greenland, Remote Sens. Environ., 112, 3739–3749, doi:10.1016/j.rse.2008.05.007, 2008.

Hall, D. K., Comiso, J. C., DiGirolamo, N. E., Shuman, C. A., Box, J. E., & Koenig, L. S.: Variability in the surface temperature and melt extent of the greenland ice sheet from MODIS. *Geophysical Research Letters, 40*(10), 2114-2120. doi: 10.1002/grl.50240, 2013.

Hanna, E., Fettweis, X., Mernild, S. H., Cappelen, J., Ribergaard, M. H., Shuman, C. A., Steffen, K., Wood, L. and Mote, T. L.: Atmospheric and oceanic climate forcing of the exceptional Greenland ice sheet surface melt in summer 2012, Int. J. Climatol., 34(4), 1022–1037, doi:10.1002/joc.3743, 2014.

Harper, J., Humphrey, N., Pfeffer, W. T., Brown, J. and Fettweis, X.: Greenland ice-sheet contribution to sea-level rise buffered by meltwater storage in firn., Nature, 491(7423), 240–3, doi:10.1038/nature11566, 2012.

Hoffman, M. J., Catania, G. A., Neumann, T. A., Andrews, L. C. and Rumrill, J. A.: Links between acceleration, melting, and supraglacial lake drainage of the western Greenland Ice Sheet, J. Geophys. Res. Surf., 116, doi:10.1029/2010JF001934, 2011.

Howat, I. M., de la Pena, S., van Angelen, J. H., Lenaerts, J. T. M. and van den Broeke, M. R.: Expansion of meltwater lakes on the Greenland Ice Sheet, The Cryosphere, 7(1), 201–204, doi:10.5194/tc-7-201-2013, 2013.

Humphrey, N. F., Harper, J. T. and Pfeffer, W. T.: Thermal tracking of meltwater retention in Greenland's accumulation area, J. Geophys. Res., 117(F1), F01010, doi:10.1029/2011JF002083, 2012.

Joughin, I., Das, S. B., King, M. a, Smith, B. E., Howat, I. M. and Moon, T.: Seasonal speedup along the western flank of the Greenland Ice Sheet., Science, 320(5877), 781–3, doi:10.1126/science.1153288, 2008.

Khan, S. A., Kjaer, K. H., Bevis, M., Bamber, J. L., Wahr, J., Kjeldsen, K. K., Bjork, A. A., Korsgaard, N. J., Stearns, L. A., van den Broeke, M. R., Liu, L., Larsen, N.K. and Muresan, I. S.: Sustained mass loss of the northeast greenland ice sheet triggered by regional warming. Nature Climate Change, 4(4), 292-299. doi: 10.1038/nclimate2161, 2014.

Koenig, L. S. and Hall, D. K.: Comparison of satellite, thermochron and air temperatures at Summit, Greenland, during the winter of 2008/09, J. Glaciol., 56(198), 735–741, 2010.

Koenig, L. S., Miège, C., Forster, R. R. and Brucker, L.: Initial in situ measurements of perennial meltwater storage in the Greenland firn aquifer, Geophys. Res. Lett., 41(1), 2013GL058083, doi:10.1002/2013GL058083, 2014.

Krawczynski, M. J., Behn, M. D., Das, S. B. and Joughin, I.: Constraints on the lake volume required for hydro-fracture through ice sheets, Geophys. Res. Lett., 36, doi:10.1029/2008GL036765, 2009.

Lampkin, D. J.: Supraglacial lake spatial structure in western Greenland during the 2007 ablation season, J. Geophys. Res., 116(F4), F04001, doi:10.1029/2010JF001725, 2011.

Lampkin, D.J., VanderBerg, J.: Supraglacial melt channel networks in the Jakobshavn Isbræ region during the 2007 melt season, Hydrol. Process., 28(25), doi: 10.1002/hyp.10085, 2013.

Langford, V. S., McKinley, A. J. and Quickenden, T. I.: Temperature dependence of the visible-near-infrared absorption spectrum of liquid water, J. Phys. Chem. A, 105(39), 8916–8921, doi:10.1021/jp010093m, 2001.

Leuschen, C.: IceBridge Snow Radar L1B Geolocated Radar Echo Strength Profiles, Boulder, Colorado, NASA DAAC at the National Snow and Ice Data Center, accessed 2014.

Luck, W.A.P.: A Model of Hydrogen-Bonded Liquids, Angewandte Chemie International Edition in English, 19(1), 28-41, 1980.

McMillan, M., Nienow, P., Shepherd, A., Benham, T. and Sole, A.: Seasonal evolution of supra-glacial lakes on the Greenland Ice Sheet, Earth Planet. Sci. Lett., 262(3-4), 484–492, doi:10.1016/j.epsl.2007.08.002, 2007.

Mote, T. L.: Greenland surface melt trends 1973-2007: Evidence of a large increase in 2007, Geophys. Res. Lett., 34, doi:L22507 10.1029/2007gl031976, 2007.

Munneke, P. K., M. Ligtenberg, S. R., van den Broeke, M. R., van Angelen, J. H. and Forster, R. R.: Explaining the presence of perennial liquid water bodies in the firn of the Greenland Ice Sheet, Geophys. Res. Lett., 41(2), 476–483, doi:10.1002/2013GL058389, 2014.

Nghiem, S. V., Hall, D. K., Mote, T. L., Tedesco, M., Albert, M. R., Keegan, K., Shuman, C. A., DiGirolamo, N. E. and Neumann, G.: The extreme melt across the Greenland ice sheet in 2012, Geophys. Res. Lett., 39(20), n/a–n/a, doi:10.1029/2012GL053611, 2012.

Ohmura, A. and 10 others: Energy and mass balance during the melt season at the equilibrium line altitude, Paakitsoq, Greenland ice sheet. Progress Report No. 1, Eidgenoss. Tech. Hochschule, Zurich, Department of Geography, 1991.

Palmer, S., Shepherd, A., Nienow, P. and Joughin, I.: Seasonal speedup of the Greenland Ice Sheet linked to routing of surface water, Earth Planet. Sci. Lett., 302, 423–428, doi:10.1016/j.epsl.2010.12.037, 2011.

Panzer, B., Gomez-Garcia, D., Leuschen, C., Paden, J., Rodriguez-Morales, F., Patel, A., Markus, T., Holt, B. and Gogineni, P.: An ultra-wideband, microwave radar for measuring snow thickness on sea ice and mapping near-surface internal layers in polar firn, J. Glaciol., 59(214), 244–254, doi:10.3189/2013JoG12J128, 2013.

Rennermalm, a. K., Smith, L. C., Chu, V. W., Box, J. E., Forster, R. R., Van den Broeke, M. R., Van As, D. and Moustafa, S. E.: Evidence of meltwater retention within the Greenland ice sheet, The Cryosphere., 7(5), 1433–1445, doi:10.5194/tc-7-1433-2013, 2013.

Rodriguez-Morales, F., Gogineni, S., Leuschen, C. J., Paden, J. D., Li, J., Lewis, C. C., Panzer, B., Alvestegui, D. G.-G., Patel, A., Byers, K., Crowe, R., Player, K., Hale, R. D., Arnold, E. J., Smith, L., Gifford, C. M., Braaten, D. and Panton, C.: Advanced Multifrequency Radar Instrumentation for Polar Research, IEEE Trans. Geosci. Remote Sens., 52(5), 2824–2842, doi:10.1109/TGRS.2013.2266415, 2014.

Selmes, N., Murray, T. and James, T. D.: Fast draining lakes on the Greenland Ice Sheet, Geophys. Res. Lett., 38, doi:10.1029/2011GL047872, 2011.

Shepherd, A., Ivins, E. R., A, G., Barletta, V. R., Bentley, M. J., Bettadpur, S., Briggs, K. H., Bromwich, D. H., Forsberg, R., Galin, N., Horwath, M., Jacobs, S., Joughin, I., King, M. A., Lenaerts, J. T. M., Li, J., Ligtenberg, S. R. M., Luckman, A., Luthcke, S. B., McMillan, M., Meister, R., Milne, G., Mouginot, J., Muir, A., Nicolas, J. P., Paden, J., Payne, A. J., Pritchard, H., Rignot, E., Rott, H., Sørensen, L. S., Scambos, T. A., Scheuchl, B., Schrama, E. J. O., Smith, B., Sundal, A. V, van Angelen, J. H., van de Berg, W. J., van den Broeke, M. R., Vaughan, D. G., Velicogna, I., Wahr, J., Whitehouse, P. L., Wingham, D. J., Yi, D., Young, D. and Zwally, H. J.: A reconciled estimate of ice-sheet mass balance., Science, 338(6111), 1183–9, doi:10.1126/science.1228102, 2012.

Sneed, W. A. and Hamilton, G. S.: Validation of a method for determining the depth of glacial melt ponds using satellite imagery, Ann. Glaciol., 52(59), 15–22, 2011.

Sundal, A. V, Shepherd, A., Nienow, P., Hanna, E., Palmer, S. and Huybrechts, P.: Evolution of supra-glacial lakes across the Greenland Ice Sheet, Remote Sens. Environ., 113, 2164–2171, doi:10.1016/j.rse.2009.05.018, 2009.

Sundal, A. V., Shepherd, A., Nienow, P., Hanna, E., Palmer, S. and Huybrechts, P.: Melt-induced speed-up of Greenland ice sheet offset by efficient subglacial drainage, Nature, 469(7331), 522–U83, doi:10.1038/nature09740, 2011.

Surdu, C. M., Duguay, C. R., Brown, L. C. and Fernandez Preto, D.: Response of ice cover on shallow lakes of the North Slope of Alaska to contemporary climate conditions (1950-2011): radar remote-sensing and numerical modeling data analysis, The Cryosphere, 8, 167-180, doi:10.5194/tc-8-167-2014, 2014.

Tedesco M, Fettweis X, Van den Broeke M, Van de Wal R, Smeets C, Van de Berg W, Serreze M, Box J.: The role of albedo and accumulation in the 2010 melting record in Greenland. Environ Res Lett 6:014005, 2011.

Tedesco, M. and Steiner, N.: In-situ multispectral and bathymetric measurements over a supraglacial lake in western Greenland using a remotely controlled watercraft, The Cryosphere, 5(2), 445–452, doi:10.5194/tc-5-445-2011, 2011.

Tedstone, A. J., Nienow, P. W., Sole, A. J., Mair, D. W. F., Cowton, T. R., Bartholomew, I. D. and King, M. A.: Greenland ice sheet motion insensitive to exceptional meltwater forcing, Proc. Natl. Acad. Sci. U. S. A., 110(49), 19719–19724, doi:10.1073/pnas.1315843110, 2013.

Ulaby, F.T., Moore, R. K., and Fung,A. K.: Microwave Remote Sensing: Active and Passive. Vol. 2. Reading, Mass: Addison-Wesley Pub. Co., Advanced Book Program/World Science Division, 1981.

Van der Veen, C. J.: Fracture propagation as means of rapidly transferring surface meltwater to the base of glaciers, Geophys. Res. Lett., 34(1), doi:10.1029/2006GL028385, 2007.

Van der Veen, C. J., Krabill, W. B., Csatho, B. M. and Bolzan, J. F.: Surface roughness on the Greenland ice sheet from airborne laser altimetry, Geophys. Res. Lett., 25(20), 3887–3890, doi:10.1029/1998GL900041, 1998.

Vernon, C. L., Bamber, J. L., Box, J. E., van den Broeke, M. R., Fettweis, X., Hanna, E. and Huybrechts, P.: Surface mass balance model intercomparison for the Greenland ice sheet, Cryosph., 7(2), 599–614, doi:10.5194/tc-7-599-2013, 2013.

Wan, Z. M., Zhang, Y. L., Zhang, Q. C. and Li, Z. L.: Validation of the land-surface temperature products retrieved from Terra Moderate Resolution Imaging Spectroradiometer data, Remote Sens. Environ., 83, 163–180, 2002.

Warren, S. G.: Optical-constants of ice from the ultraviolet to the microwave, Appl. Opt., 23(8), 1206–1225, 1984.

Wiesmann, A. and Matzler, C.: Microwave emission model of layered snowpacks, Remote Sens. Environ., 70(3), 307–316, doi:10.1016/S0034-4257(99)00046-2, 1999.

Zwally, H. J., Abdalati, W., Herring, T., Larson, K., Saba, J. and Steffen, K.: Surface melt-induced acceleration of Greenland ice-sheet flow, Science. 297(5579), 218–222, doi:10.1126/science.1072708, 2002.

Table 1. Number of buried lakes detected in each year along with the number of lakes detected per km of flightlines below 2000 m , the mean elevation and standard deviation of buried lake elevations and the percentage of buried lake below 1000 m in elevation. See Figure 6 for spatial distribution.

Year Collected	Buried Lakes Detected	Buried Lakes per 1000 km of flightlines below 2000 m	Mean Elevation (m)	Std Elevation	% of Buried Lakes Below 1000 m
2009	57	2.1	1268	290	14
2010	85	2.2	1180	399	33
2011	174	3.9	1415	295	10
2012	127	3.1	1371	332	15

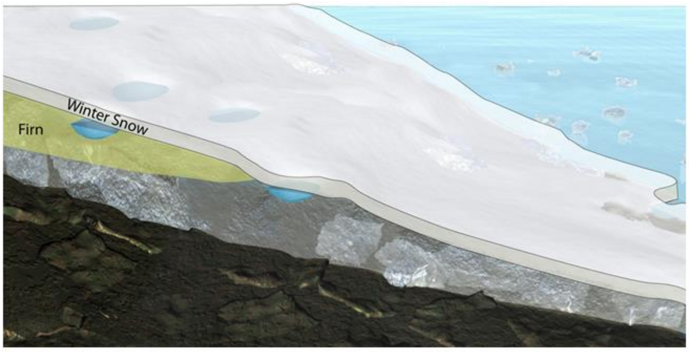

Figure 1. An illustration showing an early spring cross sectional and perspective view of buried supraglacial lakes (blue), existing under the seasonal snow layer, still filled with water after the winter season.

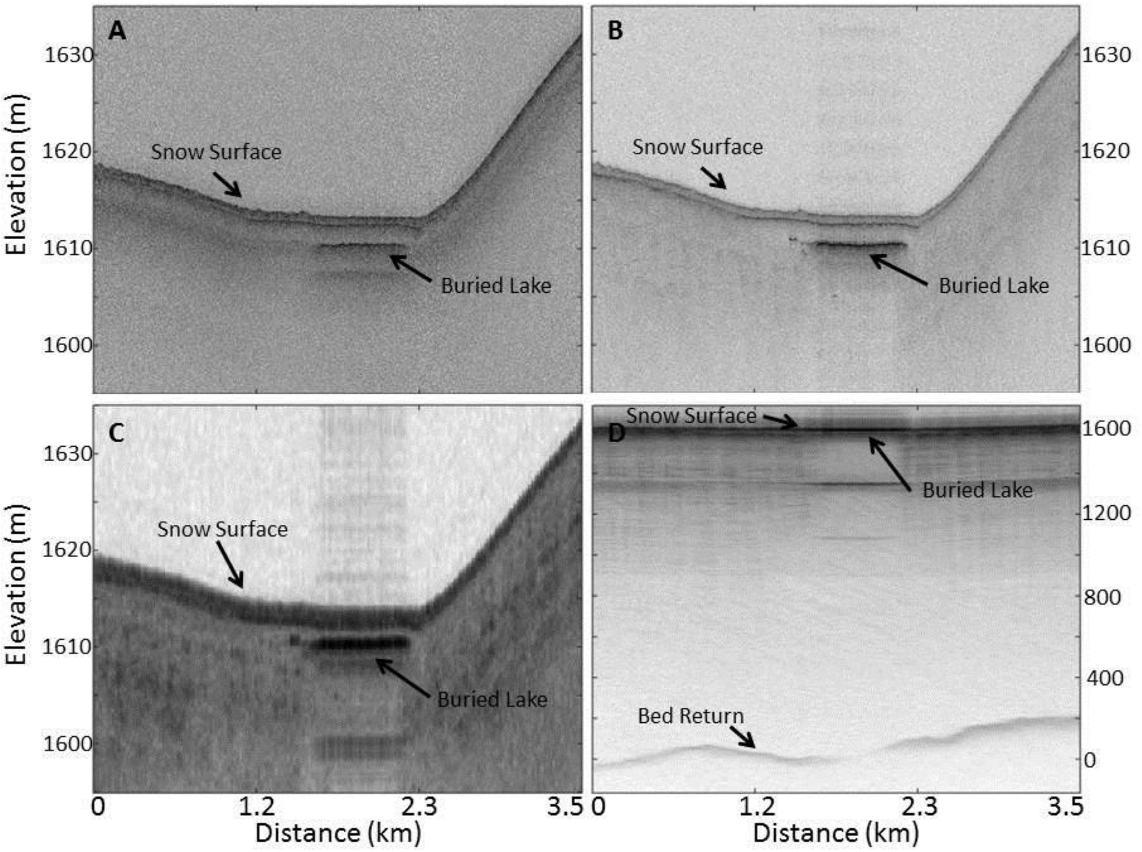

Figure 2. Radar echograms from Western Greenland (~90 km inland of Jakobshavn’s terminus) showing radar signal attenuation at multiple frequencies over a buried lake from the A) Ku-band Radar (~13-17 GHz) B) Snow Radar (~2-6.5 GHz) C) Accumulation Radar (~600-900 MHz) and D) MCoRDS Radar (~140-260 MHz).

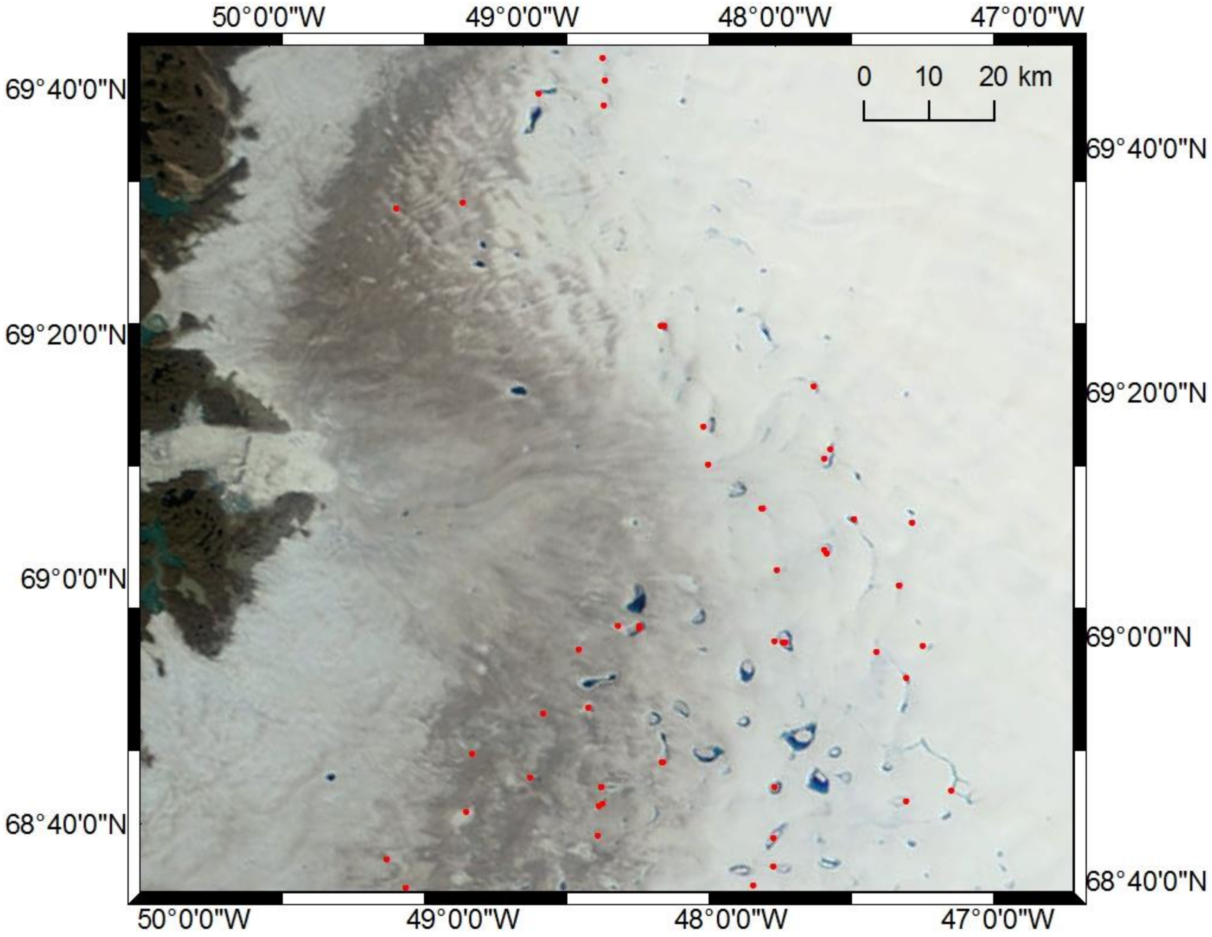

Figure 3. MODIS Rapid Response image from August 7, 2010 with buried lake detections from April-May, 2011 (red dots) overlying many of the supraglacial lakes. All buried lakes in the dataset were at some point in time visible in the MODIS imagery.

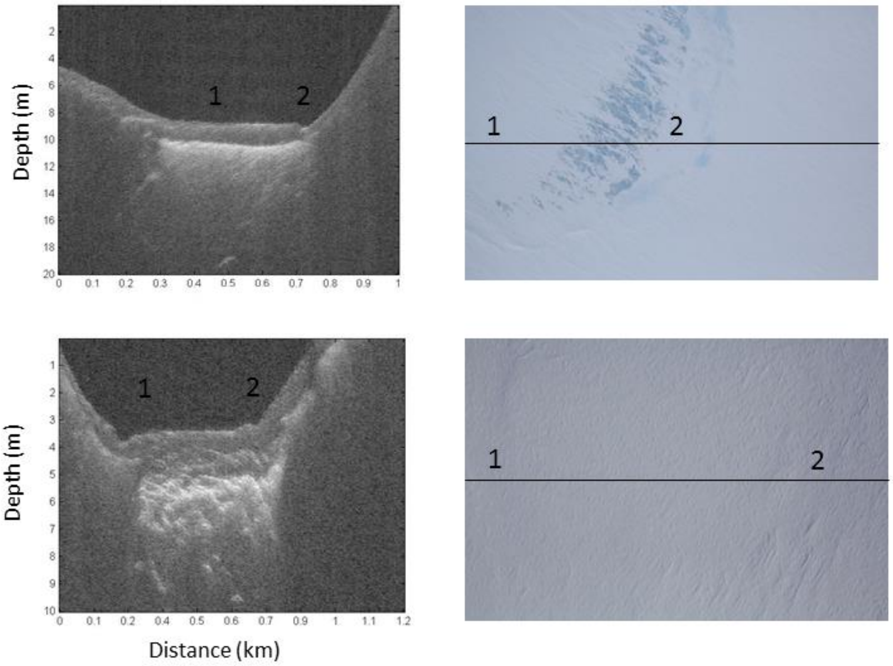

Figure 4. Snow Radar echogram of buried lakes (left) with DMS imagery of the GrIS surface (right) from: (top) a rare buried lake in Northwest Greenland (~45 km inland from the terminus of Steenstrup Glacier) with a surface expression showing darker blue where there is buried liquid water and a more turquoise, lighter blue where the lake is frozen through and (bottom) a typical buried lake in Western Greenland (~60 km inland from the terminus of Jakobshavn Isbræ) showing surface sastrugi and no detectable lake surface expression.

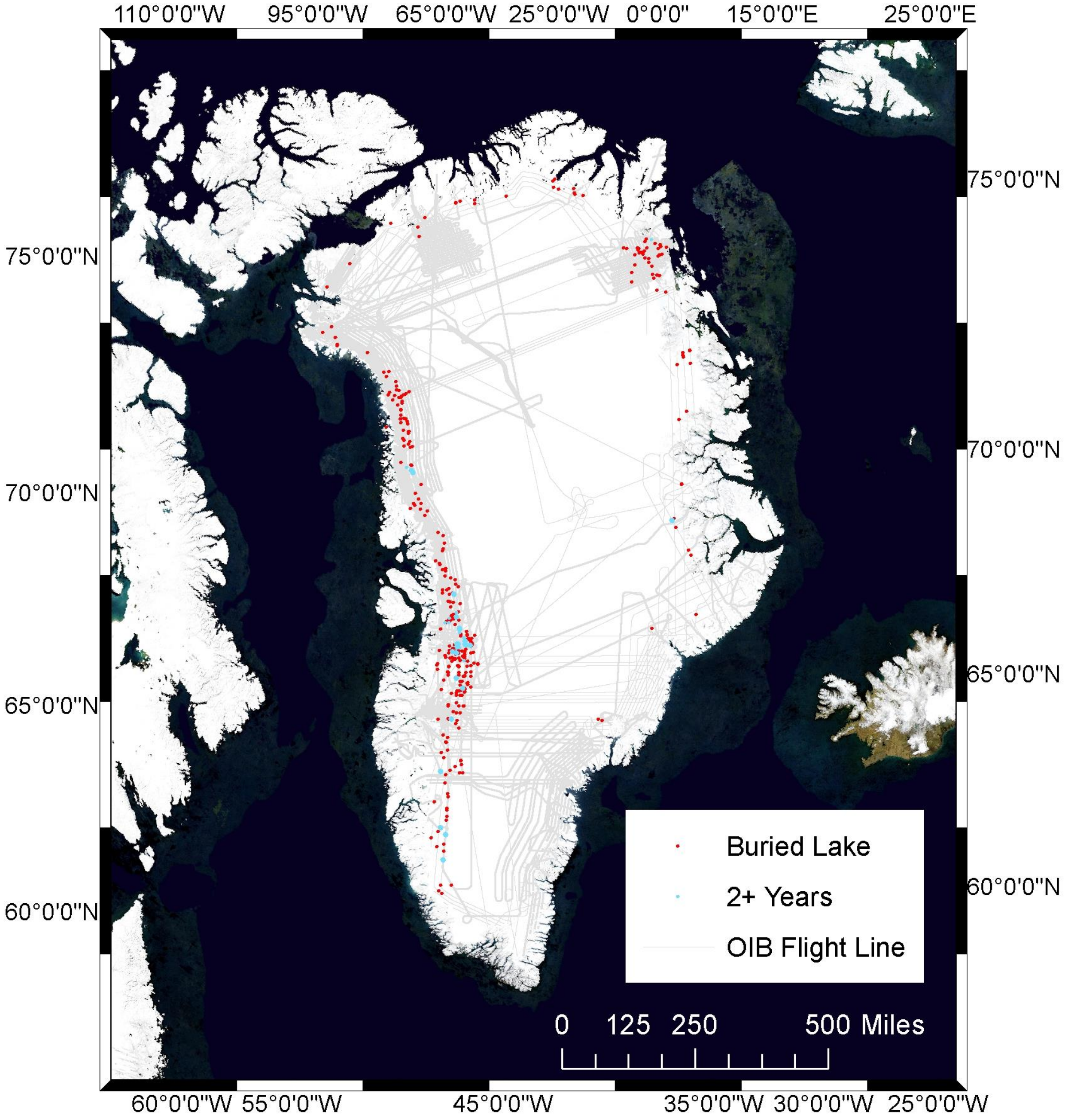

Figure 5. Locations of buried lakes (red circles) and multi-year buried lakes (blue circles) from 2009-2012 with OIB flight lines (gray lines).

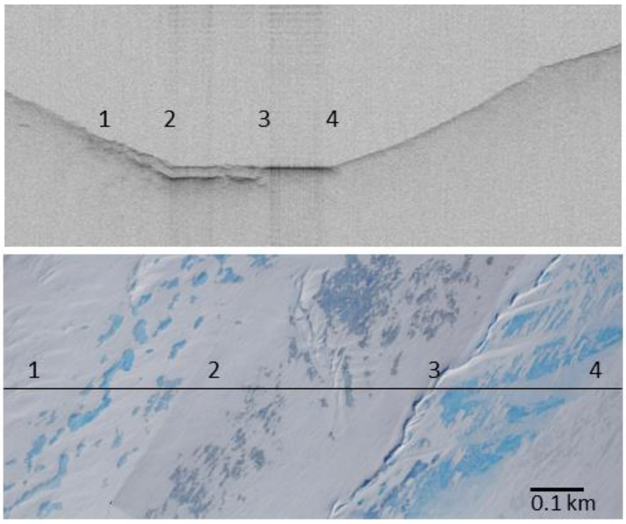

Figure 6. Snow Radar echogram (top) with DMS image of GrIS snow surface (bottom) taken on May 2, 2011 for a buried lake in North Greenland (~100 km inland from the terminus Zachariæ Isstrøm) showing from location 1 to 2 the turquoise blue refrozen lake, from 2 to 3 the darker blue retained water, a pressure ridge at 3, and from 3 to 4 surface melt caused by radiative heating at the surface of the refrozen lake edge.

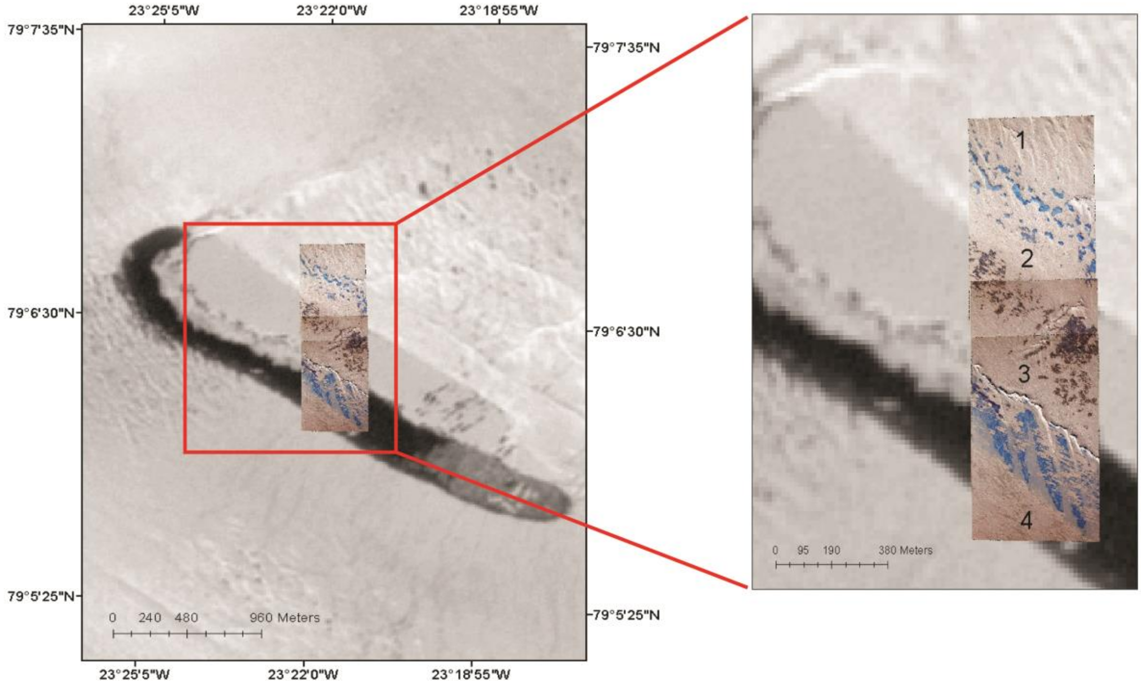

Figure 7. Image comparison of May 2, 2011 DMS image for the buried lake in Figure 6 superimposed over a Landsat ETM+ image acquired on July 19, 2011, well into the melt season, when a supraglacial lake had formed. Expanded images are of the same location over the section of the lake where the early season radar data showed initial surface melt. The lake extent correlates with the early season melt area (between locations 3 and 4) and the stored area of stored water maintained a floating ice cap into the melt season (between locations 2 and 3).

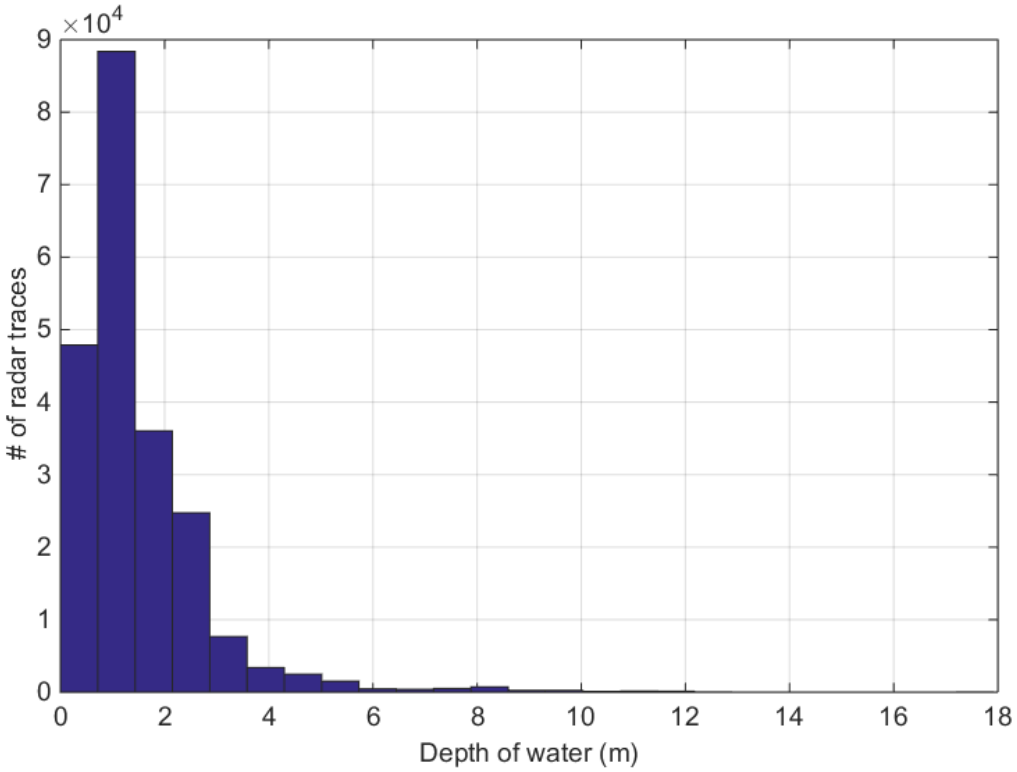

Figure 8. Histogram showing the depth of the water surface from every radar return over a buried lake from 2009-2012. Error estimates on the depth are on average 9% shallower due to uncertainties associated with the stratigraphy of density across the GrIS, which is used to convert radar travel time to depth.